

Effect of IGS baseline length on GNSS Positioning Accuracy

Rudarsko-geološko-naftni zbornik
(The Mining-Geology-Petroleum Engineering Bulletin)
UDC: 528.4
DOI: 10.17794/rgn.2023.3-7

Preliminary communication



Tarek A. Mohamed¹; Mohamed A. Yousef²; Mustafa K. Alemam¹; Yasser G. Mostafa²

¹ Mining & Metallurgical Eng. dept., Faculty of Engineering, University of Assiut, 71515, Egypt.

² Civil Eng. dep., Faculty of Engineering, University of Sohag, Egypt.

Abstract

Since the establishment of the International GNSS Service (IGS) stations, they have been used as control stations for assigning the Precise point positioning (PPP) positions using one Global Navigation Satellite System (GNSS) receiver, which has increased from day-to-day. There are some factors affecting the accuracy of PPP positioning. This research aims to investigate the relation between the IGS distance and observed field points as well as to attempt to describe that relation mathematically/statically. For the realization of that aim, two field points are fixed inside the Assiut University campus and observed successively for a session of 24 hour observation. The position of each field point is assigned with the help of each one of the available IGS station products. It must be known that these products are found after observations in three files (IGU, IGR, and final IGS), whereas IGU is used directly as real-time data (ultra-rapid), IGR (rapid) is used through (17-41 hours) after observation, and (final IGS) used after 12 – 18 days. Coordinates and point errors of each field points are computed and represented. It has been found that the errors have a positive relation with the available IGS stations distances. The relation between these distances and point positioning errors have been represented and described according to a model. The accuracy of the presented model is ($R \cong .98$, $x^2 \cong 2.5 \times 10^{-3}$).

Keywords:

GNSS stations; IGS; PPP; CDDIS; orbit files

1. Introduction

The Global Navigation satellite system (GNSS) represents a very important web for human life. It is necessary for integration into many applications so that it is becoming increasingly ingrained in human behaviour. GNSS applications have a significant impact on the development of countries. These applications include transportation (road, air, maritime, and rail), and advanced technologies (timing, scientific survey, earth observation, and network synchronization). GNSS technology is critical for the real-time prediction of critical situations and natural disasters. Furthermore, all levels of human security in our society are linked to GNSS applications (Sanou, 2013).

Differential positioning and Precise Point Positioning (PPP) are the two techniques that fall under the category of GNSS. In differential positioning, two or more receivers are used to observe the same satellites at the same time, with one or more receiver/receivers occupying known points (Bases) and the other receiver/receivers occupying the unknown point/points (Rover/Rovers). Since the unknown points' positioning coordinates

are related to the base station's positioning coordinates, the majority of observation errors can be minimized or eliminated using different processes (Horemuž and Andersson, 2006). In the end, the user receiver estimates its position relative to the reference one. Relative positioning can be achieved using either code or carrier phases. The differential positioning technique has some drawbacks, including the need for equipment (at least a pair of receivers), the requirement for simultaneous observations at both or all receivers, the limited baseline length, and reference frame inconsistency. All of these conditions make differential positioning expensive and difficult to operate, particularly in remote areas with no such infrastructure (Andrei, 2011).

In recent years, there has been a steady increase of interest in achieving high positional accuracy with a PPP. The need to reduce the cost of differential positioning using multiple receivers and save time and effort while occupying multiple stations has always pushed for faster steps to achieve higher positional accuracy using a single receiver (El-Tokhey et al., 2019). Standard Point Positioning (SPP) and PPP, which are two degrees of the Absolute Point Positioning (APP) service (based on precision), are available (Acheampong, 2008; Sunehra, 2013). PPP is a method of positioning that employs undifferenced pseudo-range and carrier phase observations

Corresponding author: Tarek A. Mohamed

e-mail address: tarek.mohamed.90@eng.aun.edu.eg

from a single high-precision dual-frequency GNSS receiver, as well as precise ephemerides and satellite clock data. This technique avoids the disadvantages of differential positioning techniques and has the potential to provide the same positioning accuracy without the need for a reference station. The success of this system will improve the operational flexibility of precise positioning using GNSS while also lowering field operational costs (Abdel-Salam, 2005).

PPP will also increase the number of GNSS-enabled applications, such as vehicle navigation, machine control, and atmospheric sensing. Also, the use of PPP in real-time GNSS applications, such as earthquake early warning which has gained traction lately (Ruckstuhl and Norris, 2009). With the development of GNSS satellite orbit and clock products, PPP could provide absolute positioning with millimetres and centimetres of precision of daily solutions for horizontal and vertical components, respectively (Gao and Chen, 2004; Hayal and Sanli, 2016). Because of its simplicity and cost-effectiveness, PPP is rising in popularity among surveyors (Zumberge et al., 1997). There are several factors that can affect the accuracy of the PPP technique such as the quality of satellite orbits and clock corrections generated from a network of global reference stations, the number of satellites, satellite geometry, observation duration, multipath and noise, receiver and antenna quality, ambiguity resolution and reference frame consistency (Kouba and Héroux, 2001). It is remarked that there are differences in the obtained results (coordinates of the same occupied field point) corresponding to the different available International Geodetic Society stations.

El-Rabbany (2002) presented several GPS point positioning methods. The PPP approach has demonstrated centimetre-to-decimetre positioning accuracy. To achieve this level of precision, precise ephemeris and satellite clock data are used, which is currently available with some latency. Many researchers and institutions, however, are developing models for predicting ephemeris and satellite clock correction, which would enable real-time PPP. Carlin et al. (2021) viewed PPP as a well-established approach for carrier phase-based navigation. Traditionally, it relies on accurate orbit and clock components to reach centimetre-level accuracy. The test study found that employing broadcast ephemerides in a PPP model is practical with modern GNSS constellations and capable of achieving accuracies in the order of a few decimeters and when correcting the signal-in-space range error (SISRE), compensation techniques are used.

Mosavi et al. (2013) estimated the receiver position using the Kalman Filter (KF) with pseudo-range data, carrier phase data, or a combination of these. Then, they presented the advantages and disadvantages of each. The accuracy achieved was 23.20 cm for the KF code observable, 20.83 cm for the KF phase observable, and 12.52 cm for the phase code observables. Chen et al. (2014) used a new GPS positioning algorithm to im-

prove single-point positioning at short observation times by combining doppler and code phase measurements. The results referred to an accuracy of 24 cm for an observation time of about 1 minute, and an accuracy ranging from 10 to 20 cm for an observation time of about 10 minutes. Guo et al. (2010) presented both static and kinematic testing in PPP solutions using International GNSS Service (IGS) file 5 min, the 30 s, and 5 s-interval precise satellite clock products. According to the results of the tests, the sampling rate of the IGS satellite clock has very little effect on the static PPP solution. All three types of precise satellite clock sampling intervals can satisfy mm-cm level positioning accuracy; a higher sampling rate has no significant improvement for the PPP solution.

The present work aims to study that phenomenon and investigate the relation between the distances of different IGS stations and the accuracy of field point position. In this research, the main procedures are as follows. Section 2 presents the International GNSS Service. Section 3 describes the field work and observations. Section 4 shows the processing of the observations and results. Analysis of the results and modelling are contained in Section 5. Section 6 explains the discussion of the present results. Finally, the conclusions and recommendations are written in section 7.

2. International GNSS Service

The IGS System was established in 1994 as a voluntary federation of self-funding organizations, academic institutions, and research centres from over 100 countries. The collaboration to provide the highest precision GNSS satellite orbits in the world offers free and open access to these products for scientific advancement and public benefit. It creates products that support the realization of the International Terrestrial Reference Frame (ITRF) while maintaining cost-effectiveness. Also, it works to continuously develop new products and applications through Working Groups and Pilot Projects. Thereover, it supports “geodetic research and scholarly publications” (Ogaja, 2022).

Figure 1 shows the IGS network in 2021. It consists of several CORS (Continuously Operating Reference Stations) run by numerous organizations that pool their resources under the IGS banner. The number of stations has grown rapidly to 509 stations as of January 31, 2021 (Villiger et al., 2020, 2021).

The GPS, GLONASS, Galileo, BeiDou, QZSS, and SBAS constellations are all tracked by the IGS global network of continuously operating geodetic quality stations. It's known that Data Centers, Analysis Centers, the Central Bureau, the Governing Board, and Associate Members, as well as Pilot Projects and Working Groups, are all included in the operational structure of IGS. Both IGS Global Data and numerous Regional Data Centers store raw station data. The Analysis Center Coordinator,

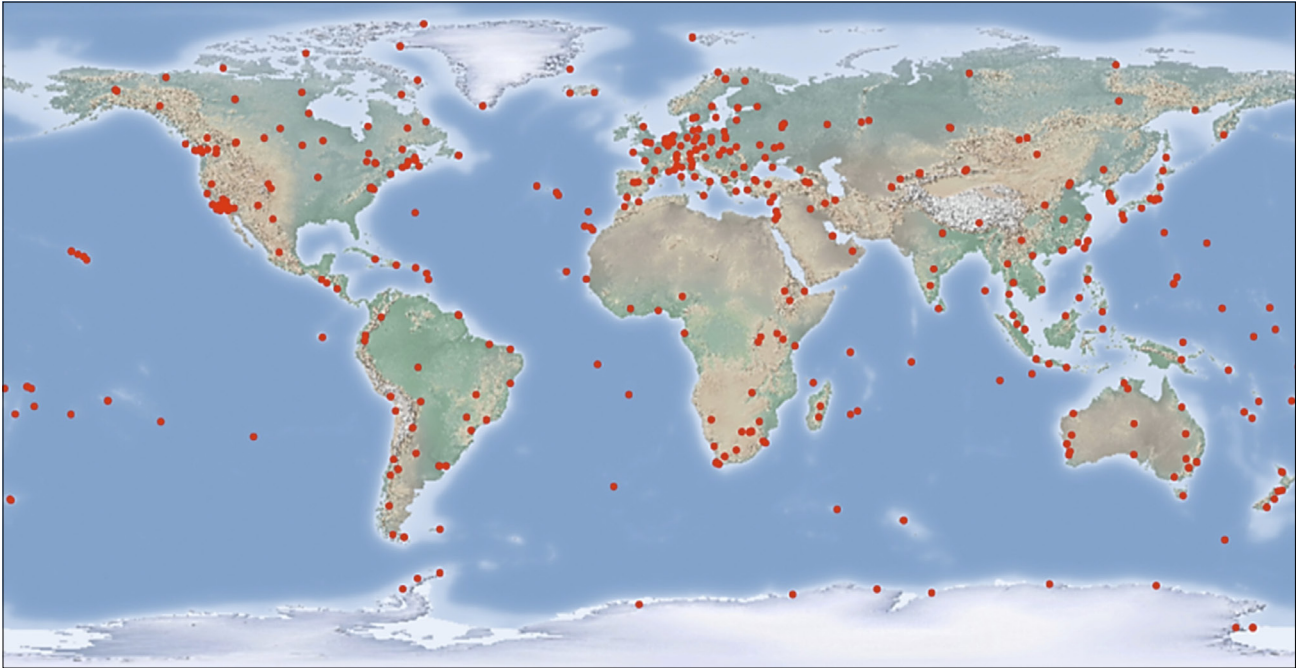


Figure 1: The 509 IGS stations as of January 31, 2021. (from Villiger et al., 2021)

Table 1: IGS orbits and clock accuracy. (from TUSAT and Ozyuksel, 2018)

| Type | | Latency | Updates | Sample Interval |
|-------------------------------------|--------------------|---------------|-----------------------|---------------------------|
| Broadcast | orbits | Real-time | — | Daily |
| | Sat. clocks | | | |
| Ultra-Rapid (predicted half) | orbits | Real-time | at 03, 09, 15, 21 UTC | 15 min |
| | Sat. clocks | | | |
| Ultra-Rapid (observed half) | orbits | 3 – 9 hours | at 03, 09, 15, 21 UTC | 15 min |
| | Sat. clocks | | | |
| Rapid | orbits | 17 – 41 hours | at 17 UTC daily | 15 min |
| | Sat. & Stn. clocks | | | 5 min |
| Final | orbits | 12 – 18 days | every Thursday | 15 min |
| | Sat. & Stn. Clocks | | | Sat.: 30 s Stn.: 5 min |

who creates the official IGS combined products, receives products from the Analysis Centers regularly after they have processed the data (Dow et al., 2009). Since the advent of the IGS system, broadcast ephemeris, and final, rapid, and ultra-quick products, have all advanced significantly. After receiving and processing tracking data from GNSS networks, IGS analysis centres integrate these solutions to provide combined IGS orbit/clock products (Montenbruck et al., 2015; Springer and Hugentobler, 2001).

There are currently five different types of GNSS satellite orbit and clock products on the market. The broadcast ephemeris and IGS ultra-fast (predicted half) products are primarily intended for real-time applications, whilst the IGS rapid and final products are intended for post-processing. The nominal accuracies of broadcast orbits and clocks, according to the IGS official website

are 1 m and 5 ns, respectively. IGS produces two sorts of ultra-rapid products: one is observed half with 39% latency and the other is predicted half with no latency. Ultra-rapid observed-half and predicted-half orbits and clocks are reported to have nominal accuracy of 3 cm and 150 ps and 5 cm and 3 ns, respectively. Final and rapid orbits and clocks are said to have nominal accuracies of 2.5 cm and 75 ps, respectively in Table 1 (TUSAT and Ozyuksel, 2018).

The processing approach and maximum employed GNSS stations of the different Analyses Centers determine the latency and accuracy variances between the products. The geodetic datum of the solutions is defined by the processing of final solutions, which contains minimal limitations. This indicates that the sum of the rotations of a group of reference frame stations must be zero. The solution's reference frame is free in scale and origin



Figure 2: Study area with both field stations (TADN and MECH).

for the most part. The reference frame is determined in the quick and ultra-rapid solutions by closely restricting the 3D position of a collection of selected reference GNSS stations. Rapid and ultra-rapid products often need fewer stations than the final product due to time constraints. The broadcast ephemeris and IGS ultra-rapid (predicted half) products are transmitted without delay. Final, rapid, and ultra-rapid (observed half) IGS products have latencies of 12-18 days, 17-41 hours, and 3-9 hours, respectively. Every six hours, IGS ultra-rapid products are updated to reduce the divergence in orbit fitting over time. Each package has 24 hours of observed orbits and another 24 hours of anticipated orbits (Ogutcu, 2020).

The results are presented in the following sections including fieldwork and observations in section 3, processing of observations in section 4, and Mathematical statistical processing of results and modelling in section 5.

3. Fieldwork and observations

The study established two concrete field stations at Assuit University, it utilized a Trimble R8S geodetic GNSS receiver which is a multi-constellation and multi-frequency model.

3.1. Fieldwork

To achieve the aim of the present work, two field stations sites were selected and established inside the campus of Assuit University, Egypt. One station termed (TADN) is fixed on the building surface of the Mining and Metallurgical Engineering Department, Faculty of Engineering, and the second one termed (MECH) has been fixed on the building surface of the Mechanical Engineering Department at the same faculty. **Figure 2** shows the location of the study area with the two selected field points.

Both stations are constructed from a concrete mixture and have trapezoidal shapes. The dimensions of each station are 23.6 cm \times 22.6 cm upper surface, 27 cm \times 25.7 cm lower surface and 12.8 cm height with 5 cm depth under the ground. A groove has been made in the centre of the upper surface area for both field points. **Figure 3** shows both field sites, and the Trimble geodetic GNSS receiver setup on the “TADN” field point.

3.2. Field observation

A Trimble R8S geodetic GNSS receiver is used. The receiver is of the multi-constellation and multi-frequency model which has 440 channels. This model can track GPS, GLONASS, Galileo, BeiDou, QZSS, and NavIC (IRNSS) satellites at positioning speeds of 1 Hz, 2 Hz, 5 Hz, 10 Hz, and 20 Hz. Its positioning accuracy for the High-Precision Static survey for the R8S receiver is [3

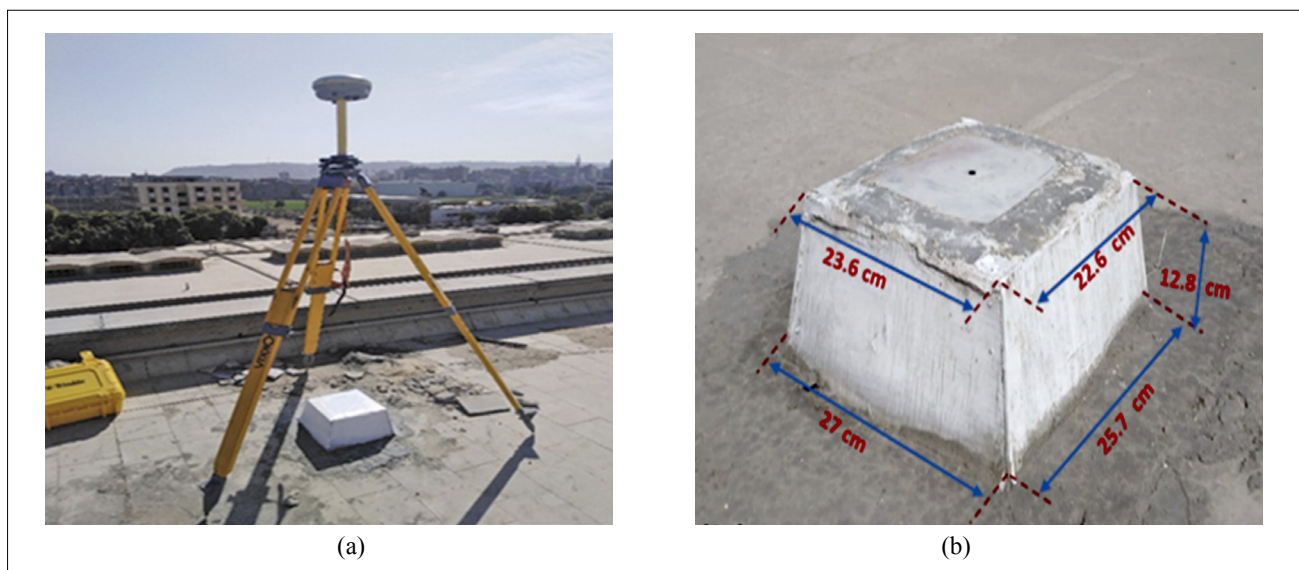


Figure 3: Field points sites a) “TADN” field station occupied with the Trimble geodetic GNSS receiver b) “MECH” Station shape and size.

mm + 0.1 ppm RMS (Horizontal)] and [3.5 mm + 0.4 ppm RMS (Vertical)]. The two stations (TADN and MECH) are occupied respectively with the GNSS receiver mentioned above at 24 hours for each, and the observations are gathered by tracking all the available satellites in view. Observation times are the GPS weeks 2195 for (TADN) and 2196 for (MECH) on January 2022. An elevation mask of 12° and a recording interval of one second are applied.

4. Processing of observations and results

As one of the four Global Data Centres (GDCs), the Crustal Dynamics Data Information System (CDDIS) supports the IGS’s GNSS data and product archiving. In this capacity, the CDDIS offers online access to the GNSS data produced by the IGS network as well as to the working group, core, and pilot project products that were created using this data. Depending on the time coverage, the CDDIS stores IGS GNSS data in three different formats: daily, hourly, and sub-hourly. The 24h of data in the daily data files, which cover the period from 00:00:00 to 23:59:30 in GPS time, is sampled every 30 seconds. Following the end of the UTC day, stations send daily files to data centres (ideally within minutes after the end of the day) (Gurtner and Estey, 2007). Daily, hourly, and sub-hourly high-rate GNSS data are stored for all sites in type-specific files: observation, which includes measurements of the code and phase, navigation (either GPS or GLONASS), which includes the broadcast ephemeris, and meteorological, which includes measurements of the temperature, pressure, and humidity made by instruments that are co-located.

The Receiver INdependent EXchange (RINEX) format is used to store all of these types of data, regardless of the sampling rate or period (Noll, 2010). Individual Analysis Centres (ACS) and Associate Analysis Centers (AACs) deliver derived products to the IGS Global Data Centers according to predetermined timetables, such as sub-daily, daily, or weekly (GDCs). These solutions are retrieved by the assigned IGS Analysis Center Coordinator (ACC) for each product, who subsequently creates a composite product that is stored at the CDDIS and the other IGS GDCs from the official website by using GPS time (weeks 2195 and 2196) and we can download the IGS orbit files. There are three types of IGS orbit and clock combination solutions: final, rapid, and ultra-rapid. The Extended Standard Product 3 (SP3c) format is used by all orbit and clock solution files (Griffiths and Ray, 2009).

4.1. Processing of observations

The processing operation of observations is accomplished through the following stages.

4.1.1. Downloading of GNSS observations

Raw data of GNSS observations for both field points (TADN and MECH) are downloaded from the receiver

Table 2: Processed coordinates of field points according to IGU product.

| IGS station | TADN point | | | | | | MECH point | | | | | | Remarks | | | |
|-------------|------------|----|---------|--------|-------|----------|------------|-------------|-------|--------|----------|----|---------|----------|------------|-------------|
| | Geodetic | | | Ground | | | Geodetic | | | Ground | | | | | | |
| | Φ | | λ | E [m] | N [m] | Φ | | λ | E [m] | N [m] | Remarks | | | | | |
| | ° | ' | | | | ° | ' | | | | ° | ' | | | | |
| RAMO | 27 | 11 | 7.88403 | 31 | 10 | 14.43404 | 318784.020 | 3008305.915 | 27 | 11 | 10.07829 | 31 | 10 | 20.23814 | 318944.749 | 3008371.117 |
| DRAG | 27 | 11 | 7.87773 | 31 | 10 | 14.42966 | 318783.897 | 3008305.723 | 27 | 11 | 10.07854 | 31 | 10 | 20.23190 | 318944.577 | 3008371.127 |
| BSHM | 27 | 11 | 7.87692 | 31 | 10 | 14.42837 | 318783.861 | 3008305.699 | 27 | 11 | 10.07889 | 31 | 10 | 20.23861 | 318944.762 | 3008371.135 |
| NICO | 27 | 11 | 7.88544 | 31 | 10 | 14.43659 | 318784.091 | 3008305.958 | 27 | 11 | 10.06984 | 31 | 10 | 20.23154 | 318944.563 | 3008370.860 |
| MERS | 27 | 11 | 7.88616 | 31 | 10 | 14.42698 | 318783.827 | 3008305.984 | 27 | 11 | 10.07949 | 31 | 10 | 20.23105 | 318944.554 | 3008371.157 |
| IZMI | 27 | 11 | 7.87498 | 31 | 10 | 14.42647 | 318783.808 | 3008305.640 | 27 | 11 | 10.07995 | 31 | 10 | 20.23049 | 318944.539 | 3008371.171 |
| ANKR | 27 | 11 | 7.88731 | 31 | 10 | 14.43852 | 318784.145 | 3008306.015 | 27 | 11 | 10.08047 | 31 | 10 | 20.22984 | 318944.522 | 3008371.187 |
| ISBA | 27 | 11 | 7.88783 | 31 | 10 | 14.43935 | 318784.168 | 3008306.030 | 27 | 11 | 10.08062 | 31 | 10 | 20.22864 | 318944.489 | 3008371.192 |
| ORID | 27 | 11 | 7.87377 | 31 | 10 | 14.44036 | 318784.190 | 3008305.597 | 27 | 11 | 10.08162 | 31 | 10 | 20.22806 | 318944.473 | 3008371.223 |
| DJIG | 27 | 11 | 7.89250 | 31 | 10 | 14.42360 | 318783.737 | 3008306.180 | 27 | 11 | 10.08641 | 31 | 10 | 20.22677 | 318944.440 | 3008371.371 |

IGS stations are arranged according to their distance from the field point.

Table 3: Processed coordinates of field points according to IGR product.

| IGS station | TADN point | | | | | | | | | | MECH point | | | | | | | | | | Remarks |
|-------------|------------|----|---------|----|----|----------|------------|-------------|----|----|------------|----|-------|-------------|------------|-------------|--|--|--|--|---------|
| | Geodetic | | | | | Ground | | | | | Geodetic | | | | | Ground | | | | | |
| | Φ | | | λ | | E [m] | N [m] | Φ | | | λ | | E [m] | N [m] | | | | | | | |
| | ° | ' | " | ° | ' | | | " | ° | ' | " | ° | | | ' | " | | | | | |
| RAMO | 27 | 11 | 7.88248 | 31 | 10 | 14.43404 | 318784.020 | 3008305.868 | 27 | 11 | 10.07271 | 31 | 10 | 20.23373962 | 318944.625 | 3008370.947 | | | | | |
| DRAG | 27 | 11 | 7.87897 | 31 | 10 | 14.43034 | 318783.916 | 3008305.761 | 27 | 11 | 10.07633 | 31 | 10 | 20.23288058 | 318944.603 | 3008371.059 | | | | | |
| BSHM | 27 | 11 | 7.87865 | 31 | 10 | 14.43008 | 318783.909 | 3008305.751 | 27 | 11 | 10.07680 | 31 | 10 | 20.23824045 | 318944.751 | 3008371.071 | | | | | |
| NICO | 27 | 11 | 7.88387 | 31 | 10 | 14.43500 | 318784.047 | 3008305.910 | 27 | 11 | 10.07711 | 31 | 10 | 20.23161975 | 318944.569 | 3008371.083 | | | | | |
| MERS | 27 | 11 | 7.88405 | 31 | 10 | 14.42927 | 318783.889 | 3008305.918 | 27 | 11 | 10.07746 | 31 | 10 | 20.23147977 | 318944.565 | 3008371.094 | | | | | |
| IZMI | 27 | 11 | 7.87783 | 31 | 10 | 14.42882 | 318783.874 | 3008305.727 | 27 | 11 | 10.07789 | 31 | 10 | 20.23060175 | 318944.541 | 3008371.108 | | | | | |
| ANKR | 27 | 11 | 7.88473 | 31 | 10 | 14.42831 | 318783.863 | 3008305.939 | 27 | 11 | 10.07814 | 31 | 10 | 20.23027494 | 318944.532 | 3008371.116 | | | | | |
| ISBA | 27 | 11 | 7.88516 | 31 | 10 | 14.42795 | 318783.853 | 3008305.953 | 27 | 11 | 10.07841 | 31 | 10 | 20.23024495 | 318944.532 | 3008371.124 | | | | | |
| ORID | 27 | 11 | 7.87672 | 31 | 10 | 14.43673 | 318784.091 | 3008305.689 | 27 | 11 | 10.07902 | 31 | 10 | 20.22999317 | 318944.525 | 3008371.143 | | | | | |
| DJIG | 27 | 11 | 7.88666 | 31 | 10 | 14.42692 | 318783.826 | 3008305.999 | 27 | 11 | 10.07935 | 31 | 10 | 20.22994982 | 318944.524 | 3008371.153 | | | | | |

Table 4: Processed coordinates of field points according to IGS product.

| IGS station | TADN point | | | | | | | | | | MECH point | | | | | | | | | | Remarks |
|-------------|------------|----|---------|----|----|----------|------------|-------------|----|----|------------|----|-------|----------|------------|-------------|--|--|--|--|---------|
| | Geodetic | | | | | Ground | | | | | Geodetic | | | | | Ground | | | | | |
| | Φ | | | λ | | E [m] | N [m] | Φ | | | λ | | E [m] | N [m] | | | | | | | |
| | ° | ' | " | ° | ' | | | " | ° | ' | " | ° | | | ' | " | | | | | |
| RAMO | 27 | 11 | 7.88166 | 31 | 10 | 14.43274 | 318783.984 | 3008305.843 | 27 | 11 | 10.07370 | 31 | 10 | 20.23471 | 318944.653 | 3008370.977 | | | | | |
| DRAG | 27 | 11 | 7.88029 | 31 | 10 | 14.43171 | 318783.955 | 3008305.801 | 27 | 11 | 10.07529 | 31 | 10 | 20.23464 | 318944.651 | 3008371.026 | | | | | |
| BSHM | 27 | 11 | 7.88002 | 31 | 10 | 14.43155 | 318783.950 | 3008305.793 | 27 | 11 | 10.07554 | 31 | 10 | 20.23590 | 318944.686 | 3008371.033 | | | | | |
| NICO | 27 | 11 | 7.88244 | 31 | 10 | 14.43318 | 318783.996 | 3008305.867 | 27 | 11 | 10.07568 | 31 | 10 | 20.23419 | 318944.639 | 3008371.038 | | | | | |
| MERS | 27 | 11 | 7.88291 | 31 | 10 | 14.43096 | 318783.935 | 3008305.882 | 27 | 11 | 10.07581 | 31 | 10 | 20.23395 | 318944.632 | 3008371.042 | | | | | |
| IZMI | 27 | 11 | 7.87891 | 31 | 10 | 14.43027 | 318783.914 | 3008305.759 | 27 | 11 | 10.07625 | 31 | 10 | 20.23351 | 318944.621 | 3008371.056 | | | | | |
| ANKR | 27 | 11 | 7.88367 | 31 | 10 | 14.43486 | 318784.043 | 3008305.904 | 27 | 11 | 10.07650 | 31 | 10 | 20.23332 | 318944.616 | 3008371.064 | | | | | |
| ISBA | 27 | 11 | 7.88384 | 31 | 10 | 14.43489 | 318784.044 | 3008305.909 | 27 | 11 | 10.07687 | 31 | 10 | 20.23268 | 318944.598 | 3008371.075 | | | | | |
| ORID | 27 | 11 | 7.87825 | 31 | 10 | 14.43551 | 318784.058 | 3008305.737 | 27 | 11 | 10.07705 | 31 | 10 | 20.23228 | 318944.587 | 3008371.081 | | | | | |
| DJIG | 27 | 11 | 7.88419 | 31 | 10 | 14.42884 | 318783.877 | 3008305.922 | 27 | 11 | 10.07754 | 31 | 10 | 20.23198 | 318944.579 | 3008371.096 | | | | | |

and fed into the processing software Trimble Business Center (TBC). Then, Raw data of GNSS observations for the available IGS stations are imported from the Crustal Dynamics Data Information System (CDDIS) for each station independently and then fed into the same software (TBC). It must be known that the IGS observations are of the same day of observations that are carried out for each one of the field points.

4.1.2. Import and downloading of known data

Geographic (Geodetic) coordinates of IGS stations are imported via Global Data Centres (GDCs). After that, Orbital data of the same observation day are downloaded from the CDDIS centre. That data includes three orbital files, each one can be downloaded separately according to a certain interval time beginning after ending the observation day. These files are known as IGU, IGR and IGS respectively depending on the length of the available range of that interval time as shown in **Table 1**.

4.1.3. Performing the processing operation

- The geographic coordinates of each IGS station are fed into the TBC program for correcting the raw coordinates of the station for one of the field points.
- In order to produce the adjusted coordinates of the considered field point in the form of adjusted IGU coordinates products, the file (IGU) is fed into the program TBC, where the field point raw observations, IGS raw observations, as well as the geographic coordinates of the IGS station, are found.
- The preceding process in (b) is performed for the same field point but taking into consideration each one of the other available IGS stations.
- All the above three phases are repeated by taking into consideration IGR and IGS files respectively instead of the IGU one.

4.2. Results of the observations

As a result of field observations and their processing and adjusting through (TBC) software as well as through the IGS data (raw and geodetic coordinates) and using the imported orbital files with the help of (CDDIS), the processed coordinates for each field point are obtained. It must be taken into consideration that coordinates for each field point are gained corresponding to each available IGS station and found in the three forms: IGU, IGR,

and IGS. **Tables 2, 3 and 4** include the resulting coordinates in the format of (Φ, λ) and E, N UTM coordinates for both field points regarding the three products (IGU, IGR, IGS) corresponding to the IGS station.

5. Mathematical statistical processing of results and modelling

To describe the relationship between the distance from the IGS stations and the spatial accuracy of the two points involved in the research, some mathematical and statistical steps have been made to develop the optimal mathematical model among the following models (linear, Polynomial, exponential, Logarithmic, Power, non-linear), where the relationship was found to be in a non-linear curve with a minimum precision value involved (1×10^{-6}).

5.1. Calculating the reference coordinates of field points.

The reference coordinates are the estimated ones which are obtained via the IGS product. The two stations are occupied respectively with the GNSS receiver at 24 hours for each, and the observations are gathered by tracking all the available satellites in view. These coordinates are assigned in this research by taking into consideration all the available IGS stations, and their coordinates are produced only in the form of the final IGS product. **Table 5** contains the processed reference coordinates for both field points in the form of geodetic and ground coordinates.

5.2. Processing of the results

To estimate the relation between IGS distance from the field point and its positional accuracy, coordinates and point errors of that point are computed for the three IGS products (IGU, IGR, and IGS). Coordinate errors are expressed in the form of coordinate differences between the coordinates of the field point resulting through each individual IGS station and the reference coordinates resulting through all the considered IGS stations for the same field point.

Tables 6 and 7 include the calculations of coordinates and point errors regarding the distances from IGS stations at the three products for both field points.

The following **Figures 4 and 5** show the errors at both field points in relation to the IGS station distance respectively.

Table 5: Reference coordinates of both points (TADN and MECH).

| Field point | Geodetic | | | | | | Ground | | Remarks |
|-------------|----------|----|----------|-----------|----|----------|------------|-------------|---------|
| | Φ | | | λ | | | E [m] | N [m] | |
| | ° | ' | " | ° | ' | " | | | |
| TADN | 27 | 11 | 7.88109 | 31 | 10 | 14.43227 | 318783.970 | 3008305.826 | |
| MECH | 27 | 11 | 10.07442 | 31 | 10 | 20.23522 | 318944.667 | 3008370.999 | |

Table 6: Errors at TADN station against IGS station distance.

| Station ID | DISTANCE, [KM] | Errors [m] | | | | | | | | | Remarks |
|------------|----------------|------------|-------|-------|-------|-------|-------|-------|-------|-------|---|
| | | IGU | | | IGR | | | IGS | | | |
| | | DE | DN | PE | DE | DN | PE | DE | DN | PE | |
| RAMO | 515.4859 | 0.050 | 0.090 | 0.103 | 0.049 | 0.042 | 0.065 | 0.013 | 0.017 | 0.022 | Reference coordinates are 318783.970 E and 3008305.826 N |
| DRAG | 637.5162 | 0.074 | 0.102 | 0.126 | 0.054 | 0.064 | 0.084 | 0.016 | 0.024 | 0.029 | |
| BSHM | 722.7974 | 0.109 | 0.127 | 0.167 | 0.061 | 0.074 | 0.096 | 0.021 | 0.033 | 0.038 | |
| NICO | 907.1307 | 0.121 | 0.132 | 0.179 | 0.076 | 0.084 | 0.114 | 0.025 | 0.041 | 0.048 | |
| MERS | 1080.1969 | 0.144 | 0.158 | 0.214 | 0.082 | 0.092 | 0.123 | 0.035 | 0.057 | 0.067 | |
| IZMI | 1300.3903 | 0.163 | 0.186 | 0.247 | 0.097 | 0.099 | 0.138 | 0.056 | 0.066 | 0.087 | |
| ANKR | 1416.4615 | 0.175 | 0.189 | 0.257 | 0.108 | 0.114 | 0.156 | 0.072 | 0.078 | 0.107 | |
| ISBA | 1445.9557 | 0.198 | 0.205 | 0.285 | 0.117 | 0.127 | 0.173 | 0.073 | 0.084 | 0.111 | |
| ORID | 1815.4245 | 0.219 | 0.228 | 0.317 | 0.121 | 0.136 | 0.182 | 0.088 | 0.089 | 0.125 | |
| DJIG | 2120.5280 | 0.234 | 0.355 | 0.425 | 0.145 | 0.174 | 0.226 | 0.093 | 0.097 | 0.134 | |

Table 7: Errors at MECH station against IGS station distance.

| Station ID | DISTANCE, [KM] | Errors [m] | | | | | | | | | Remarks |
|------------|----------------|------------|-------|-------|-------|-------|-------|-------|-------|-------|--|
| | | IGU | | | IGR | | | IGS | | | |
| | | DE | DN | PE | DE | DN | PE | DE | DN | PE | |
| RAMO | 515.3293 | 0.082 | 0.118 | 0.144 | 0.042 | 0.052 | 0.066 | 0.014 | 0.022 | 0.026 | Reference coordinates are 318944.667 E and 300837.999 N |
| DRAG | 637.3637 | 0.090 | 0.128 | 0.156 | 0.064 | 0.060 | 0.087 | 0.015 | 0.027 | 0.031 | |
| BSHM | 722.6596 | 0.095 | 0.136 | 0.166 | 0.084 | 0.072 | 0.111 | 0.019 | 0.034 | 0.039 | |
| NICO | 907.0298 | 0.103 | 0.139 | 0.174 | 0.098 | 0.084 | 0.129 | 0.028 | 0.039 | 0.048 | |
| MERS | 1080.0914 | 0.112 | 0.158 | 0.194 | 0.102 | 0.095 | 0.139 | 0.034 | 0.043 | 0.055 | |
| IZMI | 1300.3705 | 0.128 | 0.172 | 0.214 | 0.126 | 0.109 | 0.166 | 0.046 | 0.057 | 0.074 | |
| ANKR | 1416.3796 | 0.145 | 0.188 | 0.238 | 0.134 | 0.117 | 0.178 | 0.051 | 0.065 | 0.083 | |
| ISBA | 1445.7851 | 0.178 | 0.193 | 0.263 | 0.135 | 0.125 | 0.184 | 0.069 | 0.076 | 0.103 | |
| ORID | 1815.4436 | 0.194 | 0.224 | 0.296 | 0.142 | 0.144 | 0.202 | 0.080 | 0.082 | 0.114 | |
| DJIG | 2120.4852 | 0.227 | 0.372 | 0.436 | 0.143 | 0.154 | 0.210 | 0.088 | 0.097 | 0.131 | |

where:

- DE:** East coordinates errors, m,
- DN:** North coordinates errors, m,
- PE:** Point errors, m.

5.3. Modelling of the results

To investigate the relationship between the IGS station distance and positional accuracy and to estimate the best evaluation for this relation, a fitting has been made for point positional errors versus the different used IGS stations distance. That fitting has been made for each one of IGS products (IGU, IGR, and IGS) individually. Excel and Kaleida graph software are utilized in this respect. Values of “PE” in **Tables 6** and **7** for the mentioned products are applied. **Figures 6** and **7** show the fitting curves for positional errors (PE) according to the IGS station distances of points (TADN and MECH).

That fitting can be described through the following model:

$$PE = 1 \times 10^{-6} + m_1 \times D + m_2 \times D^{m3} \quad (1)$$

Where:

- PE* – point positional error in meters,
- D* – IGS station distance to field points in kilometres,
- m1*, *m2* and *m3* – constants which have the following values according to each one of the three products as shown in **Table 8**.

6. Discussion

PPP is a more recent method than differential positioning for static positioning with mm- to cm-level accuracy using a single geodetic-grade GNSS receiver and a precisely predetermined satellite orbit. The choice of orbit and IGS station is important for PPP because the baseline and satellite orbit have a direct impact on the station coordinates. In this study, the PPP horizontal rel-

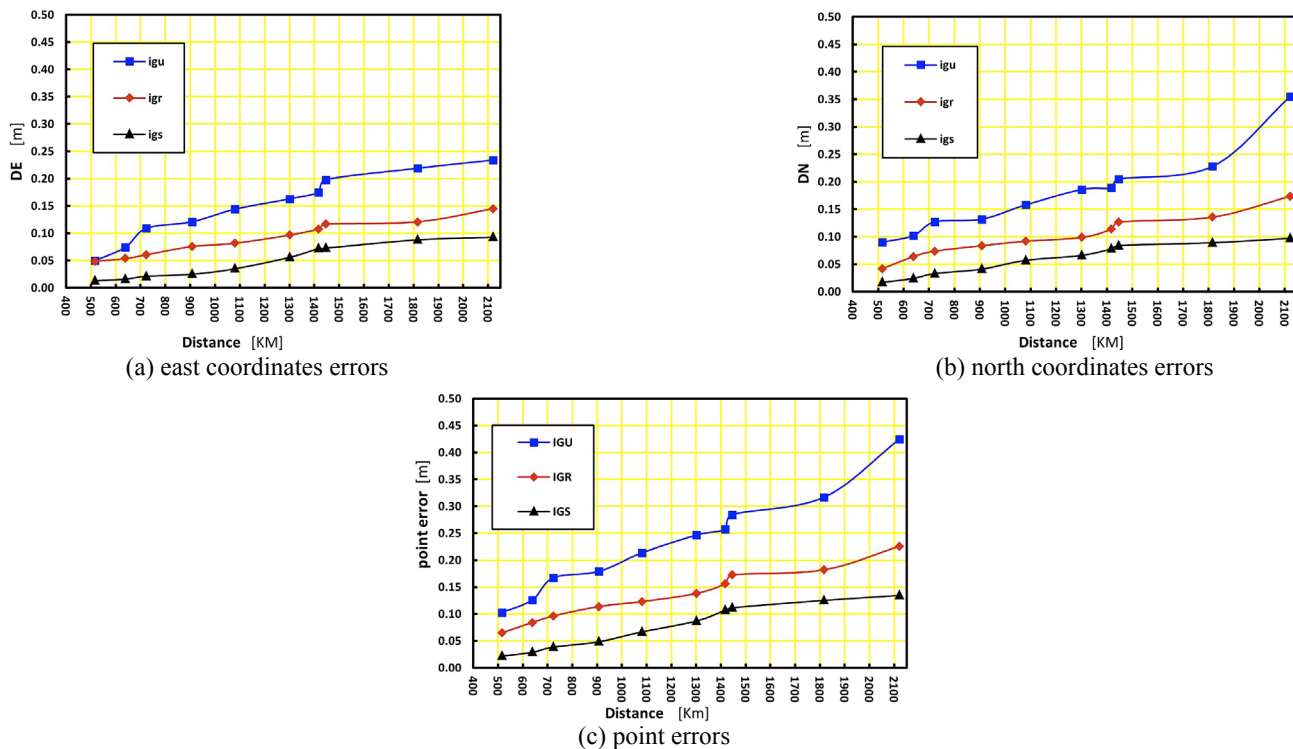


Figure 4: Errors of station TADN versus IGS station distance

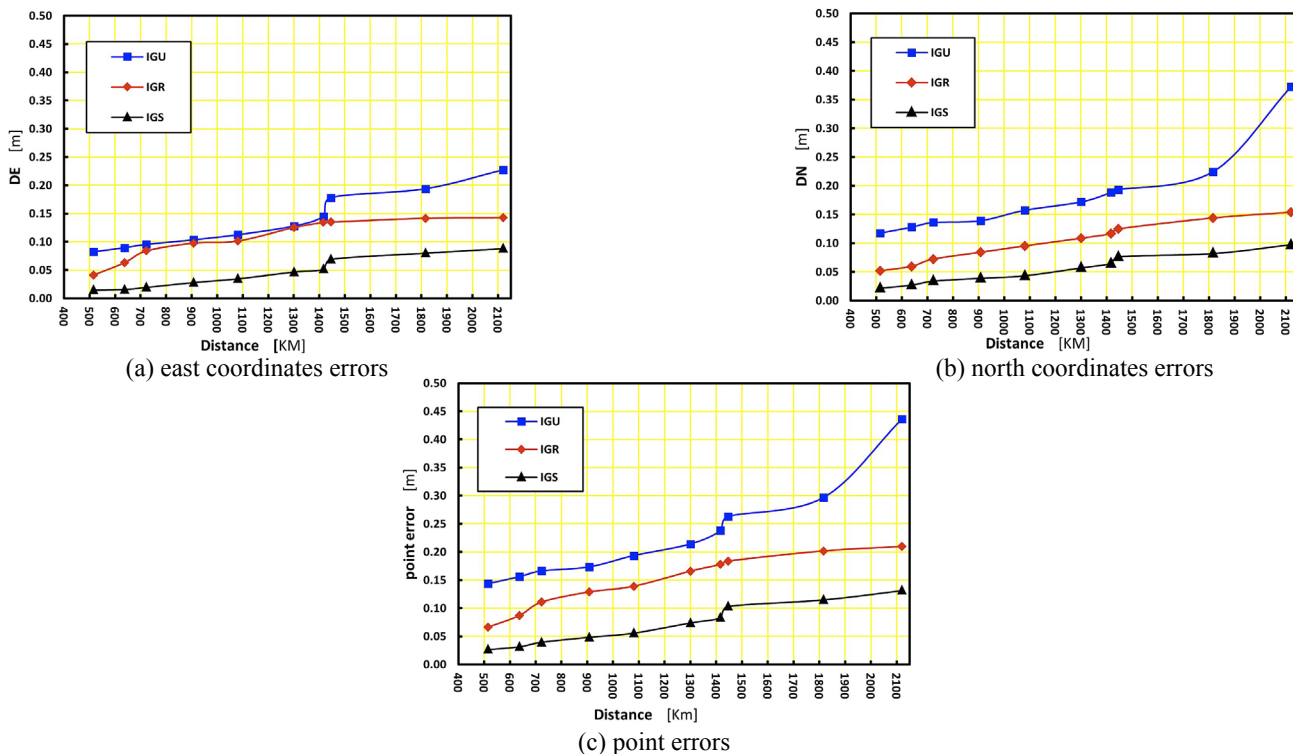


Figure 5: Errors of station MECH versus IGS station distance

ative accuracy of the widely used GNSS analysis centre IGS stations (RAMO, DRAG, BSHM, NICO, MERS, IZMI, ANKR, ISBA, ORID, and DJIG) with three different orbit files (IGU, IGR, and IGS) at two geodetic points (TADN and MECH) on January 20, 2022 (GPS week of the Year 2195 and 2196) was examined, with

their final products being taken as the true value. As shown in **Tables 6** and **7** as well as in **Figures 4** and **5** regarding TADN and MECH points, respectively, we noticed that at a minimum distance for the study area of station RAMO (baseline = 515.4859 and 515.3293 KM) to points TADN and MECH, respectively, IGU orbit

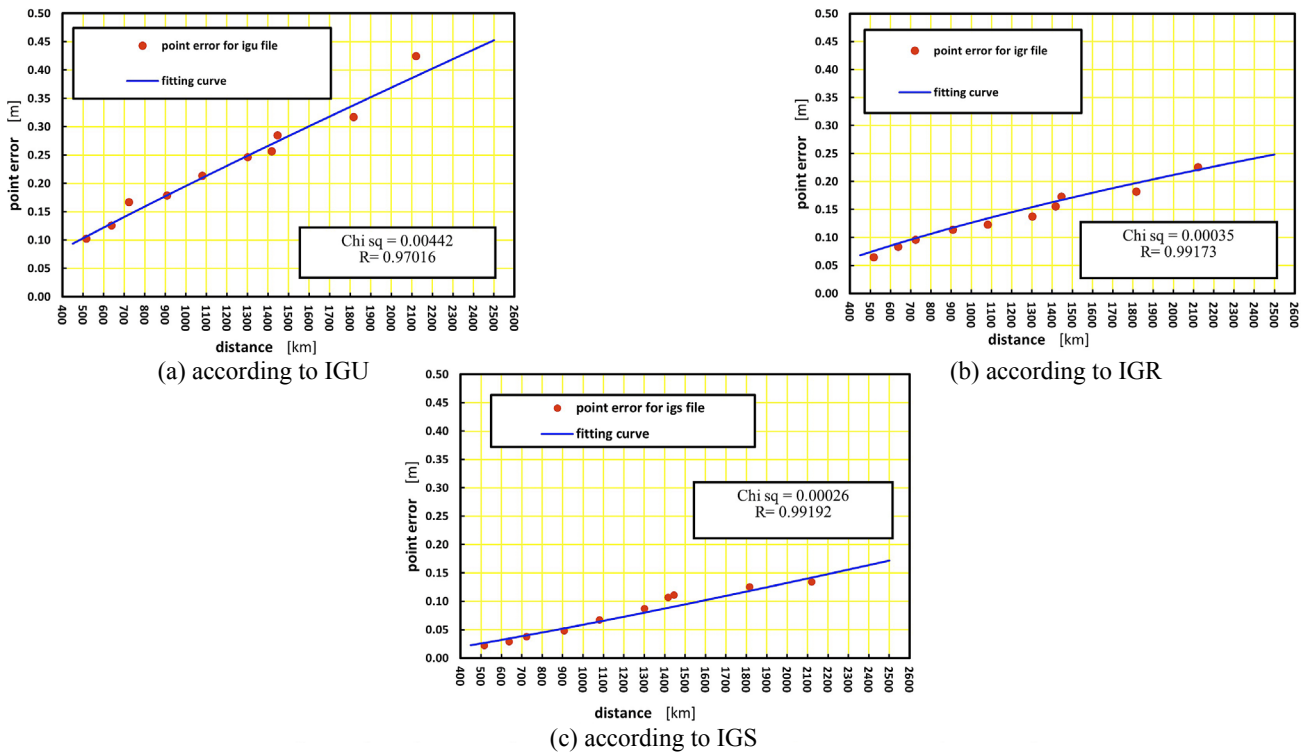


Figure 6: fitted relation between positional error and IGS distance, (field point TADN).

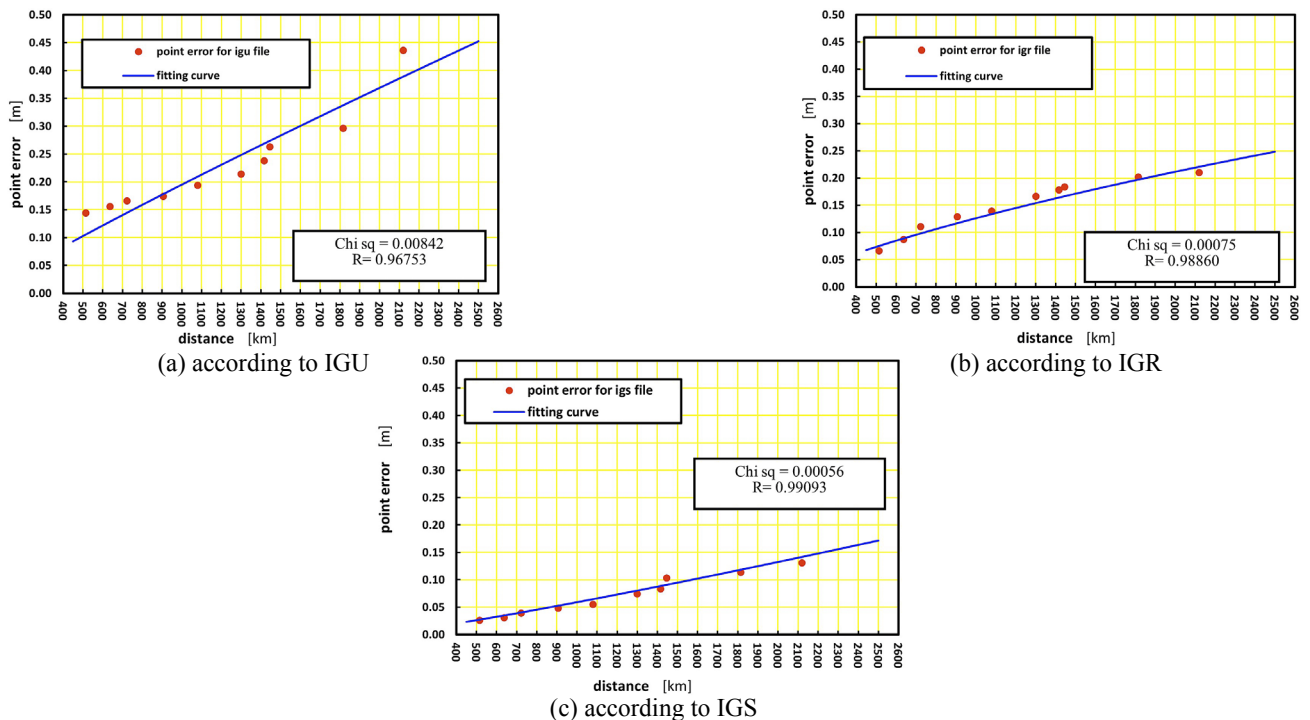


Figure 7: fitted relation between positional error and IGS distance, (field point MECH).

files east coordinate, north coordinate, and point error are 6.6 cm, 9.65 cm, and 12.35 cm, respectively. Also, the IGR orbit files' east coordinate, north coordinate, and point error are 4.55 cm, 4.7 cm, and 6.55 cm, respectively. Finally, for the TADN point, the IGS orbit files' east coordinate, north coordinate, and point error are 1.35 cm, 1.95 cm, and 2.4 cm, respectively. Then, at a

maximum distance for the study area is station DJIG (baseline = 2120.528 and 2120.4852 km) to points TADN and MECH, respectively, the IGU orbit files' east coordinate, north coordinate, and point error are 23.05 cm, 36.35 cm, and 43.05 cm. Also, the IGR orbit files' east coordinate, north coordinate, and point error are 14.4 cm, 16.4 cm, and 21.8 cm, respectively. Finally, for

Table 8: Values of the model factors

| Factor | IGU | IGR | Final IGS |
|--------|----------|-------------------------|-------------------------|
| m_1 | 0.03231 | -5.262×10^{-4} | -4.772×10^{-5} |
| m_2 | -0.03201 | 8.971×10^{-4} | 5.530×10^{-5} |
| m_3 | 1.00049 | 0.95392 | 1.09523 |

the TADN point, the IGS orbit files' east coordinate, north coordinate, and point error are 9.05 cm, 9.7 cm, and 13.25 cm, respectively. So, the east and north coordinates errors increase as the IGS station is farther. Also, point-positional errors reveal the same tendency. It is noticed that this increase in errors happens in a similar manner for each IGS product (IGU, IGR, and IGS). Through a sharp view of the coordinate and point errors, it is evident that the increase in slow rate until a distance of approximately 1500 km, then the increasing rate becomes a little more. Fitting the relation (see **Figures 6 and 7**) between the IGS distance and point error is obviously of good suitability as it verifies the important statistical requirements ($R \cong .98$, $x^2 \cong 2.5 \times 10^{-3}$).

where:

R: the correlation coefficient,

x^2 : Chi-square tests factor.

7. Conclusion and recommendations

In this paper, two locations are set up on the Assiut University campus and consecutively monitored for a period of 24 hours of observation. Each IGS station product that is available is used to determine the location of each field point. IGU (ultra-rapid) is used immediately as real-time data, IGR (rapid) is used after observation (17–41 hours), and IGS (final) is used after 12–18 days. Each field point's coordinates and point errors are calculated and shown.

The results of this work demonstrated that the PPP is; to a high extent, applicable for many surveying tasks with the help of the IGS service. This technique is particularly useful in remote areas where there are no local reference stations available, or for applications that require high accuracy but do not require real-time positioning. With a single receiver and IGS station data, establishing a network of control points with known coordinates can be used as reference points for other surveys or mapping projects, such as construction, land development, and mapping. In summary, the high accuracy and precision achievable with this approach make it a valuable tool for many different types of projects and applications. The accuracy of PPP has a positive relationship with IGS closeness from the site under consideration. Using a certain IGS product depends on the required accuracy to be achieved. The proposed predicting relation is suitable for pre-estimating the point positional accuracy at a certain IGS distance according to the used IGS product. It is recommended to study the possibility of

raising the accuracy of positioning using an IGS product (an IGU orbit file).

Acknowledgement

The authors would like to extend their sincere appreciation to the Canadian ESL Centre for their invaluable assistance with reviewing and editing.

8. References

- Abdel-Salam, M. (2005): Precise point positioning using undifferenced code and carrier phase observations. Doctorate's Dissertation, University of Calgary, Canada
- Acheampong, A. A. (2008): Developing a differential GPS (DGPS) Service in Ghana. Master's dissertation, Kwame Nkrumah University of Science and Technology, Ghana
- Andrei, C. O. (2011): Precise Point Positioning applicability for the implementation of a cadastral system in Iasi municipality. In GeoPreVi 2011, Bucharest, Romania, May 12-13. pp. 65-78.
- Carlin, L., Hauschild, A., and Montenbruck, O. (2021): Precise point positioning with GPS and Galileo broadcast ephemerides. *GPS Solut* 25, 2, 77. <https://doi.org/10.1007/s10291-021-01111-4>
- Chen, H. W., Wang, H. S., Chiang, Y. T., and Chang, F. R. (2014): A new coarse-time GPS positioning algorithm using combined Doppler and code-phase measurements. *GPS solutions*, 18, 541-551. <https://doi.org/10.1007/s10291-013-0350-8>
- Dow, J. M., Neilan, R. E., and Rizos, C. (2009): The international GNSS service in a changing landscape of global navigation satellite systems. *Journal of geodesy*, 83, 191-198. <https://doi.org/10.1007/s00190-008-0300-3>
- El-Rabbany, A. (2002): Precise GPS point positioning: the future alternative to differential GPS surveying. In *Proceedings of the ION GPS-2002*, Ontario, Canada, January, pp. 24-27.
- El-Tokhey, M., Ragheb, A., and Hassan, T. (2019): Assessment of Single and Precise Point Positioning Over Long Observational Periods. *International Journal of Engineering Research & Technology (IJERT)*, 8, 5, 178-183. <http://dx.doi.org/10.17577/IJERTV8IS050112>
- Gao, Y., and Chen, K. (2004): Performance analysis of precise point positioning using real-time orbit and clock products. *Journal of Global Positioning Systems*, 3 (1-2), 95-100.
- Griffiths, J., and Ray, J. R. (2009): On the precision and accuracy of IGS orbits. *Journal of Geodesy*, 83(3-4), 277-287. DOI 10.1007/s00190-008-0237-6
- Guo, F., Zhang, X., Li, X., and Cai, S. (2010): Impact of sampling rate of IGS satellite clock on precise point positioning. *Geo-spatial Information Science*, 13, 2, 150-156. <https://doi.org/10.1007/s11806-010-0226-9>
- Gurtner, W., and Estey, L. (2007): *Rinex-the receiver independent exchange format-version 3.00*. Astronomical Institute, University of Bern and UNAVCO, Boulder, Colorado.

- Hayal, A. G., and Sanli, D. U. (2016): Revisiting the role of observation session duration on precise point positioning accuracy using GIPSY/OASIS II Software. *Boletim de Ciências Geodésicas*, 22, 405-419. <https://doi.org/10.1590/S1982-21702016000300023>
- Horemuz, M., and Andersson, J. V. (2006): Polynomial interpolation of GPS satellite coordinates. *GPS solutions*, 10, 67-72. DOI 10.1007/s10291-005-0018-0
- Kouba, J., & Héroux, P. (2001). Precise point positioning using IGS orbit and clock products. *GPS Solutions*, 5(2), 12-28.
- Montenbruck, O., Steigenberger, P., and Hauschild, A. (2015): Broadcast versus precise ephemerides: a multi-GNSS perspective. *GPS solutions*, 19, 321-333. <https://doi.org/10.1007/s10291-014-0390-8>
- Mosavi, M. R., Azad, M. S., and EmamGholipour, I. (2013): Position estimation in single-frequency GPS receivers using Kalman filter with pseudo-range and carrier phase measurements. *Wireless personal communications*, 72, 2563-2576. <https://doi.org/10.1007/s11277-013-1166-0>
- Noll, C. E. (2010): The crustal dynamics data information system: A resource to support scientific analysis using space geodesy. *Advances in Space Research*, 45(12), 1421-1440. <https://doi.org/10.1016/j.asr.2010.01.018>
- Ogaja, C. A. (2022): *Introduction to GNSS Geodesy: Foundations of Precise Positioning Using Global Navigation Satellite Systems*. Springer Nature. <https://doi.org/10.1007/978-3-030-91821-7>
- Ogutcu, S. (2020): Performance assessment of IGS combined/JPL individual rapid and ultra-rapid products: Consideration of Precise Point Positioning technique. *International journal of engineering and geosciences*, 5, 1, 1-14. <https://doi.org/10.26833/ijeg.577385>
- Ruckstuhl, C., and Norris, J. R. (2009): How do aerosol histories affect solar “dimming” and “brightening” over Europe?: IPCC-AR4 models versus observations. *Journal of Geophysical Research: Atmospheres*, 114(D10). <https://doi.org/10.1029/2008JD011066>
- Sanou, D. A. (2013): Analysis of GNSS interference impact on society and evaluation of spectrum protection strategies. *Positioning*, 4, 2. 169-182. <http://dx.doi.org/10.4236/pos.2013.42017>
- Springer, T. A., and Hugentobler, U. (2001): IGS ultra rapid products for (near-) real-time applications. *Physics and Chemistry of the Earth, Part A: Solid Earth and Geodesy*, 26(6-8), 623-628. [https://doi.org/10.1016/S1464-1895\(01\)00111-9](https://doi.org/10.1016/S1464-1895(01)00111-9)
- Sunehra, D. (2013): Estimation of prominent global positioning system measurement errors for Gagan applications. *European Scientific Journal*, 9, 15, 68-81. <https://core.ac.uk/download/pdf/236410055.pdf>
- Tusat, E., and Ozyuksel, F. (2018): Comparison of GPS satellite coordinates computed from broadcast and IGS final ephemerides. *International Journal of Engineering and Geosciences*, 3, 1, 12-19. <https://doi.org/10.26833/ijeg.337806>
- Villiger, A., Dach, R., Schaer, S. et al. (2020): GNSS scale determination using calibrated receiver and Galileo satellite antenna patterns. *Journal of Geodesy*, 94, 93, 1-13. <https://doi.org/10.1007/s00190-020-01417-0>
- Villiger, A., Dach, R. (eds.) (2021). *International GNSS Service Technical Report 2021 (IGS Annual Report)*. IGS Central Bureau and University of Bern. Bern Open Publishing, DOI 10.48350/169536.
- Zumberge, J. F., Heflin, M. B., Jefferson, D. C., Watkins, M. M., and Webb, F. H. (1997): Precise point positioning for the efficient and robust analysis of GPS data from large networks. *Journal of geophysical research: solid earth*, 102(B3), 5005-5017. <https://doi.org/10.1029/96JB03860>

SAŽETAK

Utjecaj duljine IGS baze na točnost pozicioniranja GNSS-a

Od uspostave postaja Međunarodnoga GNSS servisa (IGS) iz dana u dan povećava se korištenje kontrolnih stanica za dodjelu položaja precizne točke (PPP) pomoću jednoga prijavnika Globalnoga satelitskog navigacijskog sustava (GNSS). Postoje neki čimbenici koji utječu na točnost PPP pozicioniranja. Cilj je ovoga istraživanja istražiti odnos između IGS udaljenosti i promatranih točaka polja te opisati taj odnos matematički i statički. Za realizaciju toga cilja dvije terenske točke fiksirane su unutar kampusa Sveučilišta Assiut i promatrane sukcesivno tijekom sesije promatranja od 24 sata. Položaj svake točke polja dodjeljuje se uz pomoć svakoga od dostupnih proizvoda IGS stanica. Bitno je napomenuti da se ti produkti nalaze u tri datoteke (IGU, IGR i konačni IGS) nakon promatranja, dok se IGU koristi izravno kao podatci u stvarnome vremenu (*ultra-rapid*), IGR (*rapid*) kroz 17 – 41 sat nakon promatranja, a konačni IGS nakon 12 – 18 dana. Koordinate i pogreške točaka svake točke polja izračunane su i prikazane. Utvrđeno je da su pogreške u pozitivnom odnosu s dostupnim udaljenostima IGS postaja. Odnos između tih udaljenosti i pogreška pozicioniranja točke prikazan je i opisan prema modelu. Točnost je prikazanoga modela $R \cong .98$, $x_2 \cong 2.5 \times 10^{-3}$.

Ključne riječi:

GNSS stanice, IGS, JPP, CDDIS, datoteke Orbit

Authors contribution

Tarek A. Mohamed (a candidate for a Master of Science degree in Mining Engineering/Geodesy Surveying) was responsible for conducting field measurements, laboratory operations analysis, and assisting in the presentation and interpretation of the findings. The concept and methodology were developed by **Mohamed A. Yousef** (an Associate Professor Emeritus in Mining Engineering/Geodesy Surveying), who also outlined the requirements of IGS stations, assisted in the analysis of field measurements, and reviewed the submitted paper. **Yasser G. Mostafa** (an Associate Professor in Civil Engineering/Engineering Surveying) drafted the introduction, assisted in the interpretation of the results, and prepared the paper. **Mustafa K. Alemam** (an Assistant Lecturer of Mining Engineering/Geodesy Surveying) made contributions to the introduction, participated in the discussion of the results, wrote the conclusions, and assisted in writing the draft manuscript. All authors collaborated on the entire manuscript.